XVI International Conference on Computational Plasticity. Fundamentals and Applications
COMPLAS 2021
E. Oñate, D. Peric, M. Chiumenti and Eduardo de Souza Neto (Eds)

MATERIAL MODELS FOR HIGHLY DYNAMIC METAL FORMING PROCESSES

Florian Katzmayr[†], Christian Reisinger[†], Thomas Gross[§], Stefan Sieberer[X], Wolfgang Kunze[Y], Leopold Wagner[Z] and Christian Zehetner[†*]

[†] University of Applied Sciences Upper Austria
Stelzhammerstraße 23, 4600 Wels, Austria
e-mail: christian.zehetner@fh-wels.at, web page: http://www.fh-ooe.at/

[§] Linz Center of Mechatronics GmbH
Altenbergerstraße 69, 4040 Linz, Austria
e-mail: thomas.gross@lcm.at - Web page: http://www.lcm.at

[X] Institute of Structural Lightweight Design, Johannes Kepler University Linz
Altenbergerstraße 69, 4040 Linz, Austria
e-mail: stefan.sieberer@jku.at - Web page: http://www.jku.at/ikl

[Y] Salvagnini Maschinenbau GmbH
Dr.-Guido-Salvagnini-Straße 1, 4482 Ennsdorf, Austria
e-mail: wolfgang.kunze@salvagninigroup.com - Web page: http://www.salvagnini.at

[Z] voestalpine Stahl GmbH
voestalpine-Str. 3, 4020 Linz, Austria
e-mail: leopold.wagner@voestalpine.com - Web page: http://www.voestalpine.com/ultralights/

Key words: sheet metal forming, rate-dependent plasticity, adiabatic heating, Johnson-Cook

Abstract. In industry, metal forming processes are widely used in manufacturing. For optimization, simulation is becoming more and more important. Forming processes can be efficiently analysed with the Finite Element Method. To obtain reliable results, a suitable material model that includes all important physical effects is essential, [1]. Especially, the flow curve model for the description of the plastic material behaviour is crucial for realistic results. In this work, we mainly focus on highly dynamic forming processes like bending or punching.

First, a dynamic flow curve model for mild steel has been selected according to the literature. To use the model for forming processes with high strain rates, the temperature is considered in addition to the strain rate for modelling the adiabatic heating effect. The selected dynamic flow curve model was then implemented as a user subroutine in the Finite Element software ABAQUS. After verifying this subroutine with a unit test on one Finite Element, the material has been calibrated. For this sake, static and dynamic tensile tests as well as in-plane torsion tests have been performed. As an important material type in sheet metal production, DC01 has been chosen. The parameters of the material model have been identified according to [2]. Outcome of this work is a calibrated material, ready to use for simulation of industrial sheet metal forming applications.

1 Introduction

When forming processes are represented by Finite Element (FE) models, the reliability of the simulation results significantly depends on the used material model. Several aspects must be taken into account like elastic and plastic behavior represented by the flow curve with all relevant influence parameters. These models differ in the considered physical effects and mathematical formulation.

In the literature, there is a large number of flow curve models. Dynamic models such as Johnson-Cook [3], Zerilli-Armstrong [4] or Cowper-Symonds [5] are based on quasi-static flow curve models, considering dynamic effects of strain-rate or temperature with multiplicative or additive terms. Quasi-static flow curve models like Hollomon [6], Ludwik [7] and Gosh [8] are widely used in FE simulation due to their simplicity. These models are based on exponential functions.

In this work a material model has been selected and calibrated to represent the rate-dependent elasto-plastic behavior relevant for sheet metal bending and punching. In these forming processes the plastic behavior is characterized by the flow curve as obtained by uni-axial tensile tests. The flow curve describes the stress as a function of plastic strain, strain rate and temperature.

Goal is to calibrate one material model for both, bending and punching simulations. Therefore, the model must represent the material behavior over a large range for strain and strain rate. Due to the high local strain rates during punching, the adiabatic heating effect also must be considered. To consider this thermal effect, depending on the strain rate, the flow curve model has been implemented as a user subroutine in the FE software ABAQUS.

Finally, the coefficients of the material model are determined for the mild steel DC01 which is frequently used in sheet metal applications. Static and dynamic material tests have been performed for this purpose. For the future, the calibration of a damage and failure model is also planned as an extension of the material model. This will allow to simulate the effect of material separation which is necessary for the simulation of punching or cutting processes.

2 Rate-dependent plastic flow curve

In the literature, the Johnson-Cook model is frequently used to describe the plastic behavior of metals under large strain, high strain rates and temperature. This phenomenological constitutive model describes the relation of Cauchy stress σ (true stress) and the Hencky strain ε (logarithmic strain, true strain). For strains lower than the yield stress, Hooke's law describes the linear relation of stress and strain as $\sigma = E\varepsilon$ with the Young modulus E.

After exceeding the yield stress, the plastic strain ε_{pl} is the difference of total strain ε and the elastic strain $\frac{\sigma}{E}$, i.e. $\varepsilon_{pl} = \varepsilon - \frac{\sigma}{E}$. In the plastic domain the Johnson-Cook model describes the stress as a function of plastic strain, plastic strain rate $\dot{\varepsilon}_{pl} = \frac{\mathrm{d}}{\mathrm{d}t}\varepsilon_{pl}$

and temperature T as

$$\sigma\left(\varepsilon_{pl}, \dot{\varepsilon}_{pl}\right) = \underbrace{\left(A + B\varepsilon_{pl}^{n}\right)}_{\text{hardening}} \underbrace{\left[1 + C \ln\left(\frac{\dot{\varepsilon}_{pl}}{\dot{\varepsilon}_{pl,0}}\right)\right]}_{\text{strain rate}} \underbrace{\left[1 - \left(\frac{T - T_r}{T_m - T_r}\right)^{m}\right]}_{\text{thermal softening}}, \tag{1}$$

where A, B, C, n and m are coefficients to be determined by experiments [3]: A is the quasi-static yield stress, B is the strength coefficient, n is the hardening exponent, C the strain rate sensitivity parameter, m is the temperature coefficient, T_r is the reference temperature, and T_m is the melting temperature.

The first term in Eq. (1) describes the hardening at the reference strain rate $\dot{\varepsilon}_{pl,0}$. The second term represents the effect of the strain rate and the third one the influence of thermal softening. Therefore, the effect of adiabatic heating can be considered. Note, that the first term of the Johnson Cook model (hardening) coincides with the model of Ludwik [7].

In the literature, there are several modifications of the Johnson-Cook model. For example, Huh-Kang [9] proposes a modification in which a quadratic part is added to the strain rate term:

$$\sigma\left(\varepsilon_{pl}, \dot{\varepsilon}_{pl}\right) = \left(A + B\varepsilon_{pl}^{n}\right) \left[1 + C_1 \ln\left(\frac{\dot{\varepsilon}_{pl}}{\dot{\varepsilon}_{pl,0}}\right) + C_2 \ln\left(\frac{\dot{\varepsilon}_{pl}}{\dot{\varepsilon}_{pl,0}}\right)^{2}\right] \left[1 - \left(\frac{T - T_r}{T_m - T_r}\right)^{m}\right]. \tag{2}$$

Instead of C in Eq. (1), now two coefficients C_1 and C_2 must be identified by material tests to calibrate the strain rate influence. Compared to the classical Johnson-Cook formulation, the quadratic term in Eq. (2) enables a better fit of the strain rate effect to experimental over a wider range of $\dot{\varepsilon}_{pl}$. This is essential for our goal to apply the material model for processes with quite different strain-rates like bending and punching.

3 ADIABATIC HEATING EFFECT

In highly dynamic forming processes, thermal softening due to adiabatic heating must be considered in the material model. To avoid complex thermomechanical coupled simulations, which are very time-consuming, the adiabatic temperature increase dT can be calculated according to [10] as

$$dT = \frac{\beta}{\rho c_p} \sigma d\varepsilon_{pl}, \tag{3}$$

where the Taylor-Quinney coefficient β describes the proportion of plastic work that is converted into heat. According to [10], this coefficient is usually assumed to be constant for metals and set to $\beta = 0.9$. Furthermore, the temperature increase depends on the density ρ and the specific heat capacity c_p. The latter can be assumed to be constant in a limited temperature range.

As mentioned above, the material model is intended to be used over a wide range of strain rates. However, at low strain rates and large deformations, Eq. (3) highly

overestimates the temperature increase, which is physically not correct. Reason is the difference of time constants for the mechanical and thermal process. Consequence is an isothermal process for low strain rates, so that the adiabatic effects do not play a role. To model the transition range from isothermal to adiabatic conditions, the Taylor-Quinney coefficient must be considered as a function of the strain rate as

$$dT = \frac{\beta\left(\dot{\varepsilon}_{pl}\right)}{\rho c_p}\sigma d\varepsilon_{pl}. \tag{4}$$

With the strain rate dependent Taylor-Quinney coefficient $\beta\left(\dot{\varepsilon}_{pl}\right)$ the transition from isothermal to adiabatic conditions can be modeled. In [10], three different transition models are presented. All three models give approximately the same results.

In this paper, the transition is modeled in a simplified form using a transition strain rate $\dot{\varepsilon}_C$. Only for higher strain rates the adiabatic term is considered in the material model:

$$\sigma\left(\varepsilon_{pl}, \dot{\varepsilon}_{pl}\right) = \begin{cases} \left(A + B\varepsilon_{pl}^n\right)\left[1 + C_1 \ln\left(\frac{\dot{\varepsilon}_{pl}}{\dot{\varepsilon}_{pl,0}}\right) + C_2 \ln\left(\frac{\dot{\varepsilon}_{pl}}{\dot{\varepsilon}_{pl,0}}\right)^2\right]\left[1 - \left(\frac{T - T_r}{T_m - T_r}\right)^m\right], & \dot{\varepsilon}_{pl} > \dot{\varepsilon}_C \\ \left(A + B\varepsilon_{pl}^n\right)\left[1 + C_1 \ln\left(\frac{\dot{\varepsilon}_{pl}}{\dot{\varepsilon}_{pl,0}}\right) + C_2 \ln\left(\frac{\dot{\varepsilon}_{pl}}{\dot{\varepsilon}_{pl,0}}\right)^2\right], & \dot{\varepsilon}_{pl} <= \dot{\varepsilon}_C \end{cases} \tag{5}$$

and the temperature is computed with Eq. (4).

4 ABAQUS SUBROUTINE

For the numerical analysis, the FE software ABAQUS has been chosen. Using the material model according to Eqs. (4) and (5) is only possible with a user subroutine. VUHARD, [11], is used to implement the modified Johnson-Cook Huh-Kang model, Eq. (2). With the latter, an isotropic plastic material behavior depending on strain, strain rate and temperature can be defined by setting the parameters appropriately. Stress, strain and strain rate as well as the equivalent strain $\bar{\varepsilon}_{pl}$ and strain rate $\dot{\bar{\varepsilon}}_{pl}$ are provided by ABAQUS, and accessible in the user subroutine, [11]. Therefore, the effort for writing code is low. Figure 1 shows the flowchart of the subroutine, i.e. the equivalent stress is computed by inserting the equivalent strain and strain rate into Eq. (5). Note, that this subroutine is executed at all element integration points for which the corresponding material law has been selected.

To test the subroutine, a single element test with one three-dimensional element of type C3D8R has been performed with ABAQUS. The element is based on linear interpolation functions, reduced integration, and hourglass control was used. As boundary conditions the nodes on one side are pinned, and on the second side the velocity is prescribed. The simulation was performed with four different amplitudes of the velocity. As parameters for this test, the coefficients A, B, n, C_1, C_2 and m are taken from [12] and the transition strain rate was set to $\dot{\epsilon}_C = 0.1\ s^{-1}$ for these numerical experiments.

The results compared to the analytical solution can be seen in Figure 2. The equivalent plastic Hencky strain is plotted on the abscissa and the calculated equivalent stress is plotted on the ordinate. First of all, it is obvious that for higher deformation speeds

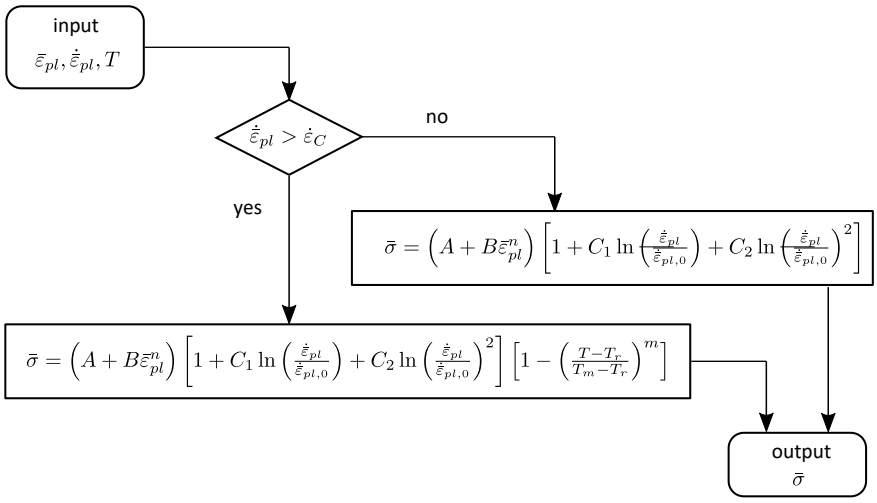

Figure 1: Flowchart of the user subroutine

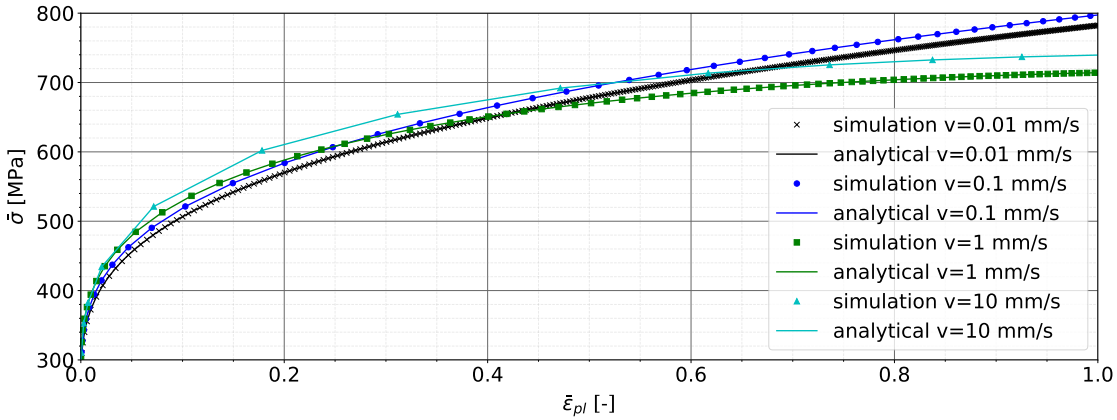

Figure 2: Comparison between simulation and analytical calculation

the stress increases. This effect results from the higher hardening depending on the strain rate. It can also be seen that for the two higher velocities ($v = 1\ mm/s$ and $v = 10\ mm/s$) the flow curve softens in the region of large strains. This softening effect is caused by adiabatic heating. Furthermore, the FE results show a very good agreement with the analytical results. Thus, the unit test demonstrates that the modelled effects are correctly reproduced by the user subroutine. In a next future step, a transition model instead of a transition strain rate could be implemented as described in [10].

5 PARAMETER IDENTIFICATION FOR MILD STEEL DC01

The parameters of the presented material model are adapted for the mild steel DC01. First, the material tests are described in sections 5.1 and 5.2. Subsequently, the parameter identification is based on [2]. The hardening parameters are identified in section 5.3 and the rate sensitivity in section 5.4.

5.1 Quasi-static tensile and in-plane torsion tests

These two kinds of tests are used to determine the flow curve for the reference strain rate $\dot{\varepsilon}_{pl,0}$. In our experiments the reference strain rate is $\dot{\varepsilon}_{pl,0} = 0.001$, which corresponds to quasistatic conditions with good approximation. For such low strain-rates, the process is isotherm ($\dot{\varepsilon}_{pl,0} < \dot{\varepsilon}_C$), so that Eq. (5) reduces to the Ludwik equation, [7]:

$$\sigma\left(\varepsilon_{pl}\right) = A + B\varepsilon_{pl}^{n}, \qquad \text{for } \dot{\varepsilon}_{pl} = \dot{\varepsilon}_{pl,0}. \tag{6}$$

The tensile tests have been performed according to DIN EN ISO 6892-1:2009. It is well-known that the strains are limited by the necking effect. This limitation can be overcome by in-plane torsion tests, [13], allowing to determine the flow curve also for strains higher than the uniform strain. This is essential for the considered industrial processes of bending and punching.

The tests have been performed at Johannes Kepler University, and the results are shown in Figure 3. There is a very good coincidence between the two test methods. Note that in a tensile test, there is a uni-axial state of stress until the uniform strain (ultimate stress) is reached. In contrast, torsional shear stresses occur in the torsion test. Thus, material anisotropy would cause discrepancies of the results of the tensile and in-plane torsion test. However, for our sheets of DC01, this effect was not observed, and it seems that anisotropy does not play a role for this material

For identifying the coefficients in Eq. (6) the flow curve is considered as follows: For $\varepsilon_{pl} < 0.15$ the result of the tensile test is used, for $0.15 < \varepsilon_{pl} < 0.175$ the curves from both tests are averaged, and for $\varepsilon_{pl} > 0.175$ the result of the torsion test is used to describe hardening. The outcome is represented by the black curve in Figure 3.

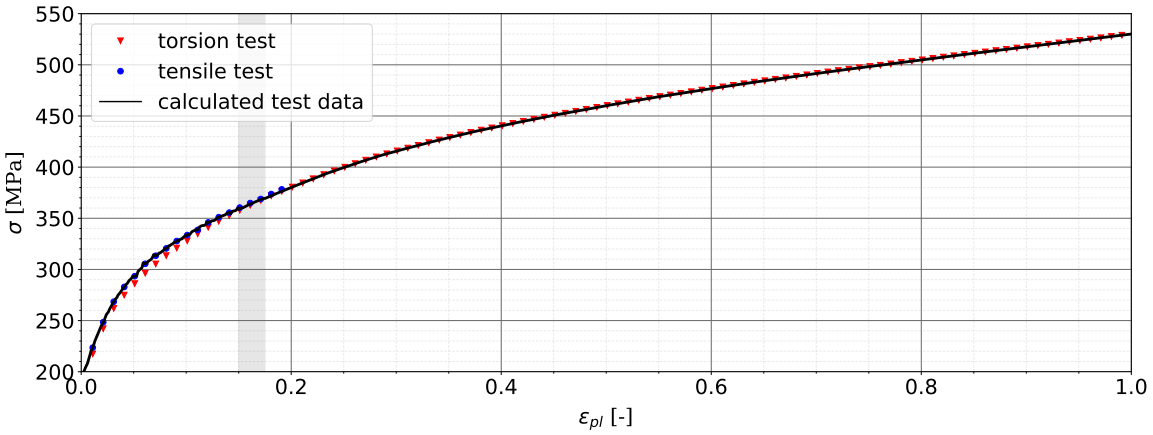

Figure 3: Quasistatic flow curves obtained by tensile and torsion tests

5.2 Dynamic compression tests

These tests are performed to calibrate the strain rate sensitivity of the flow model, i.e. the second and third term in Eq. (1). The second term represents the hardening

as a function of the strain rate, and the third term the thermal softening, because the material heats up at higher strain rates. Both terms must be taken into account to correctly represent the strain rate sensitivity.

To fully identify the Johnson-Cook model, material tests are carried out at different strain rates. Because the considered strain rates are so high that tensile tests do not give representative results, compression tests were planned for the material DC01. However, delays occurred during the execution of the tests, also as a consequence of the Covid lock-downs. Thus, the data was not available on time.

To estimate and represent the effects of strain rate and thermal softening, existing data for the material DC05 are used at this point. From our experience, this material shows a very similar behavior like DC01. The tolerance windows of these two materials in terms of mechanial properties overlap, with DC05 being the superior steel grade in terms of formability, i.e. lower yield strength, higher tensile elongation, smaller ultimate tensile strength window, etc. [14]. The compression test results for DC05 were taken from [15]. Figure 4 shows the flow curves for three different strain rates. Also, the quasi-static flow curve for DC01 is drawn.

Note, that this workaround has been done for a first estimation of the effect. Of course, dynamic compression tests are also planned for the material DC01, such that in the near future a consistent data set for DC01 should be available.

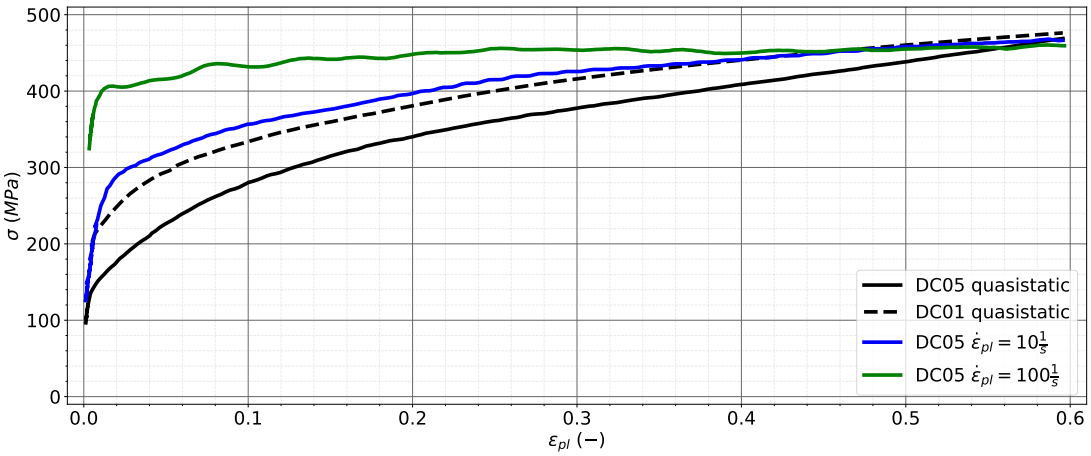

Figure 4: Flow curves DC05 obtained by compression tests

5.3 Determination of strain hardening: parameters A, B and n (DC01)

The coefficient A in Eq. (6) is the yield stress which is a standard result of a tensile test, and can be directly read from Figure 3. The coefficients B and n can be identified from the experimental data by curve fitting. It is helpful to transform the exponential Eq. (6) to a linear one by applying the logarithm as

$$\ln(\sigma - A) = n \ln(\varepsilon_{pl}) + \ln(B). \tag{7}$$

Eq. (7) shows a linear relationship between $\ln(\sigma - A)$ and $\ln(\varepsilon_{pl})$. Subsequently, a linear regression is performed to determine the coefficients B and n. Figure 5 shows the linear fit on the left, and the comparison of the experimental flow curve with the regression on the right, showing a good agreement.

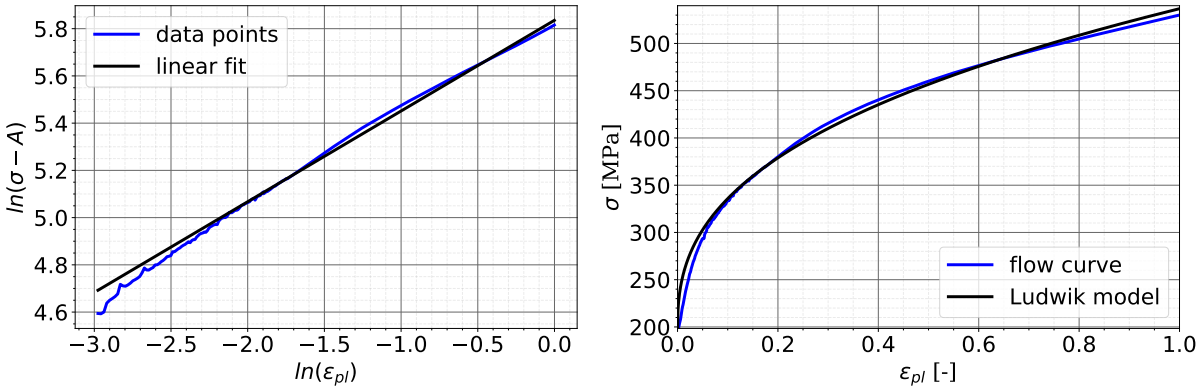

Figure 5: Determination B and n Ludwik flow curve model

5.4 Determination of rate sensitivity: Parameters C and m (DC05)

After determining the parameters A, B and n from the quasi-static flow curve (black line in Figure 4), the parameter C can be determined for the compression tests with higher strain rates. For this sake, Eq. (1) is reformulated to

$$\sigma\left(A + B\varepsilon_{pl}^{n}\right)^{-1}\left[1 - \left(\frac{T - T_r}{T_m - T_r}\right)^{m}\right]^{-1} = 1 + C\ln\left(\frac{\dot{\varepsilon}_{pl}}{\dot{\varepsilon}_{pl,0}}\right), \tag{8}$$

yielding a linear relationship between the term on the left hand side and $\ln\left(\frac{\dot{\varepsilon}_{pl}}{\dot{\varepsilon}_{pl,0}}\right)$. Now, a first order regression can be used to find the coefficient C. As the parameter m must also be determined, an iterative approach is applied. Note, that the temperature T of the material was not experimentally determined during the quasistatic and the dynamic compression tests. Therefore, it is estimated by using Eq. (3). The identification is done with the following procedure:

- Selection of an initial value for C and m
- Iterative determination of the coefficients
  1. Calculation of the adiabatic temperature using Eq. (3)
  2. Determination of m using the least square method (curve fitting)
  3. Determination of C for fixed m with a linear regression using Eq. (8)

In Figure 6, the comparison of the measured data with the regression can be seen. In our industrial application, the regions of higher strains are more relevant, so that for curve fitting only the highlighted range $\varepsilon_{pl} = [0.1; 0.6]$ has been considered.

For the quasi-static case, we obtain a very good approximation. For $\dot{\varepsilon}_{pl} = 10$ there are slight differences. For our industrial bending process, in which the strain rates are in this order of magnitude the approximation is very good. For $\dot{\varepsilon}_{pl} = 100$, the estimation is also acceptable.

Figure 7 shows the regression results without taking into account thermal softening. Comparing both figures it is obvious that this effect must be considered.

The results highlight the influence of the strain rate and the temperature on the hardening behaviour, which can be reasonably represented by the Johnson-Cook model for mild steels.

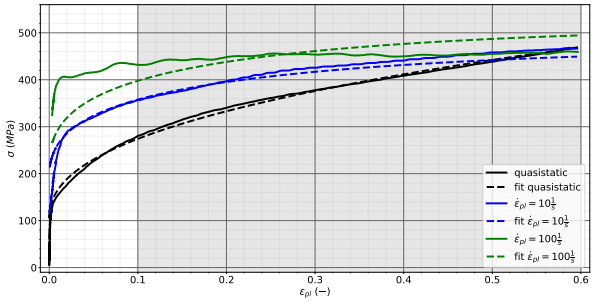

Figure 6: Identified flow curves with consideration of thermal softening, DC05

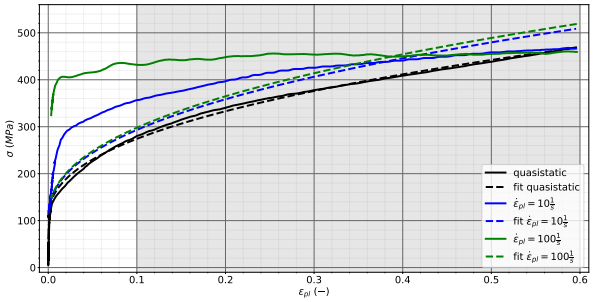

Figure 7: Identified flow curves without consideration of thermal softening, DC05

Finally, the linear fit of strain rate sensitivity with converged values for C and m is shown in Figure 8 on the left. It can be seen that with a linear regression the strain rate sensitivity is already well represented. A higher order regression as given in Huh-Kang [9], Eq. (2) does not lead to any improvement for this particular material and the considered strain rates. The right graph in Figure 8 shows the estimated adiabatic temperature increase for the different strain rates: For the quasi-static test, there is no temperature increase because it is performed slowly enough so that the generated heat can be transferred to the environment. For tests with a high strain rate, the thermal time constant is too low, and there is an increase of the temperature.

6 CONCLUSIONS

In this work, a flow curve model for the simulation of bending and punching processes was selected from the literature, i.e. the Johnson-Cook model modified by Huh-Kang in Eq. (5). This model considers strain hardening, strain rate sensitivity and adiabatic heating in case of high strain rates. Goal was to calibrate a material model for application to processes with low and high strain rates, and to implement it in ABAQUS. Only in case of high strain rates the adiabatic heating effect is relevant, for low rates the process can be considered as isotherm. This distinction requires the user subroutine VUHARD in ABAQUS. The user subroutine was written and verified by a single element test.

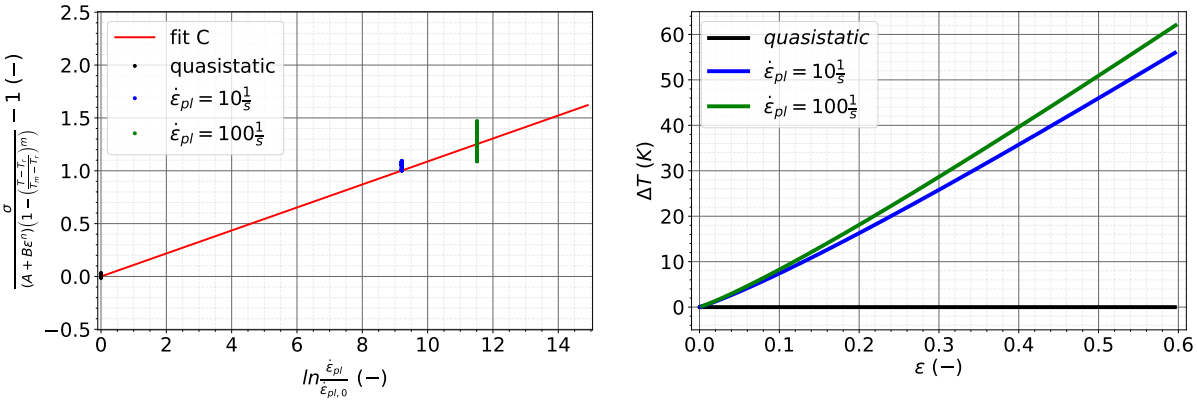

Figure 8: Determination C, DC05

Second goal was to calibrate the parameters of the material model, based on quasi-static tensile and in-plane torsion tests as well as dynamic compression tests. Mild steel DC01 has been selected as frequently used material in industries. Because compression tests for DC01 have not yet been available, existing data from DC05 have been used for a first estimation of rate sensitivity and thermal softening.

Next planned step is to calibrate the strain rate sensitivity and temperature term for DC01. For this purpose, compression tests are already scheduled with main focus on the strain rates relevant for our industrial bending process, but also beyond as relevant for punching and cutting. The analysis and evaluation framework for this task already exists as outcome of this paper. Subsequently, it is also planned to calibrate a damage and failure model for this material, allowing also the simulation of material separation as it occurs in punching and cutting applications.

7 ACKNOWLEDGEMENT

This work has been supported by the COMET-K2 “Center for Symbiotic Mechatronics” of the Linz Center of Mechatronics (LCM) funded by the Austrian federal government and the federal state of Upper Austria.

REFERENCES

[1] Zehetner, C., Reisinger, C., Kunze, W., Hammelmüller F., Eder, R., Holl, H. and Irschik, H. High-quality sheet metall production using a model based adaptive approach. *Procedia Computer Science* (2021), **180**:249-258.

[2] Murugesan M. and Jung D.W. Johnson Cook Material and Failure Model Parameters Estimation of AISI-1045 Medium Carboon Steel for Metal forming Applications. *Materials 12* (2019), **12**:609.

[3] Johnson, G.R. and Cook, W.H. Fracture characteristics of three metals subjected to various strains, strain rates, temperatures and pressures. *Engineering fracture mechanics* (1985), 21, 1, 31-48.

[4] Zerilli, F.J. and Armstrong, R.W. Dislocation-mechanics based constitutive relations for materal dynamic calculations. *J. Appl. Phys* (1987), 61(5): 1816-1825.

[5] Cowper, G.R. and Symonds, P.S. Strain hardening and strain rate effects in the impact loading of cantilever beams. *Brown University Appl. Math. Report* (1958), 28: 1-46.

[6] Hollomon, J.H. Tensile deformations. *Trans. Metall. Soc.* (1945), AIME 162: 268-290.

[7] Ludwik, P. *Elemente der Technologischen Mechanik*, Springer Verlag, (1909).

[8] Gosh, A. The influence of strain hardening and strain rate sensitivity on sheet metal forming. *J.Enger. Mater. Technol., Trans. ASME* (1977), 264-274.

[9] Kang, W.J., Cho, S., Huh, H. and Chung, D.T. Modified Johnsoon Cook model for vehicle body crashworthiness simulation. *Int. J. Veh. Des.* (1999) **21**: 424-435.

[10] Larour, P. *Strain rate sensitivity of automotive sheet steels: influence of plastic strain, strain rate, temperature, microstructure, bake hardening and pre strain. Thesis (Phd).* Rheinisch-Westfälische technische Hochschule Achen, (2010).

[11] *Abaqus Documentation*, Dassault Systems Simulia Corp., (2018).

[12] Schwer, L. Optional Strain-Rate Forms for the Johnson Cook Constitutive Model and Role of Parameter Epsilon_0. *6th European LS-DYNA Users Conference*, (2007).

[13] Wagner, L., Gross, T., Gruber, P.G., Grillenberger, M., Schagerl M. *Application of the in-plane torsion test in an industrial enviroment - recent advances and remaining challenges*. Conference Paper of the 12th Forming Technology Forum, Herrsching, Germany, (2019).

[14] Standard, D.I.N. *Cold rolled low carbon steel flat products for cold forming—Technical delivery conditions*, German version EN 10130, DIN Deutsches Institut für Normung eV, 14s, (2006).

[15] Grillenberg, M. *Charakterisierung von Hochleistungswerkstoffen für den Leichtbau unter dynamischer Drucklast, Thesis (Phd).* Johannes Kepler Universität Linz, (2020).